ICP22, and computer-fitting a pair of normal distributions to the resulting histograms. The relative areas of the two fitted curves give the relative Y and O populations in each fraction. Figure 2d shows measurement of the O fraction sorted from the sonicated ethanol-fixed cells of Fig. 2b; the Y fraction is shown in Fig. 2e. Their photographic superposition, which should be compared to Fig. 2a, is shown in Fig. 2f. Analysis shows 95, 87, and 82 percent purity of O fractions for protocols 1, 2, and 3, respectively. The purities of Y fractions were 72, 83, and 80 percent, respectively.

Two problems currently prevent use of sorted sperm for fertilization: sorting rates are low and the stained cells are not viable. Even if vital staining techniques are developed and sorting rate is increased to that attainable with current instrumentation (about 10^3 cells per second), use of sorted sperm for inseminations in vivo will not be widespread since several million cells are required for one insemination. New instrumentation with dramatically higher sorting rates might alter this situation. Application to fertilization in vitro, where the required number of sperm is significantly lower, is more probable.

For the immediate future, flow sorting of *M. oregoni* sperm offers the possibilities of directly addressing the question of haploid expression of genes linked to sex chromosomes and efficiently searching for biochemical markers that discriminate the two sperm populations. If found, a marker might be useful for bulk separation of viable sperm, perhaps by using an antibody to bind one population to a column while allowing the other to pass through. If there is a Y-specific *M. oregoni* marker that is conserved across species, it would have general application to mammalian sex selection. In the absence of a common marker, extension to other species will require sorting of biochemically well-preserved sperm differing in DNA content by 3 to 4 percent. This will be more difficult for the human than for agriculturally important species since the human DNA content difference is at the low end of the mammalian range and the heterogeneity of human sperm nuclear condensation presents greater interference to precise staining.

DANIEL PINKEL
BARTON L. GLEDHILL
SUZANNE LAKE
DIANE STEPHENSON
MARVIN A. VAN DILLA

Biomedical Sciences Division, Lawrence Livermore National Laboratory, University of California, Livermore 94550

References and Notes

1. For an overview of the status and possibilities of sex selection by semen manipulation, see R. P. Amann and G. E. Seidel, Eds. *Prospects for Sexing Mammalian Sperm* (Colorado State Univ. Press, Boulder, 1982). The contribution by R. J. Ericsson reviews various proposed techniques including centrifugation, sedimentation, electrophoresis, motility, and surface antigens. He lists eight U.S. patents issued for sperm separation. The contribution by M. L. Meistrich compares the expected physical differences between X and Y sperm to the resolution of current laboratory procedures.
2. J. F. Moruzzi, *J. Reprod. Fertil.* **57**, 319 (1979).
3. F. J. Otto, U. Hacker, J. Zante, J. Schumann, W. Göhde, M. L. Meistrich, *Histochemistry* **62**, 249 (1979).
4. D. Pinkel, S. Lake, B. L. Gledhill, M. A. Van Dilla, D. Stephenson, G. Watchmaker, *Cytometry* **3**, 1 (1982).
5. In none of these samples, from five separate sources using six different methods, did the percentage of X sperm differ from 50 percent. Data will be published when the study is completed.
6. Moruzzi (*2*) reports 8.8 percent, based on length measurements. Our flow cytometric measurements (Fig. 2a) yield 9.27 ± 0.11 percent.
7. S. Ohno, J. Jainchill, C. Stenius, *Cytogenetics* **2**, 232 (1963).
8. E. Lifschytz, in *Edinburgh Symposium on the Genetics of the Spermatozoon*, R. A. Beatty and S. Gluecksohn-Waelsch, Eds. (Univ. of Edinburgh Press, Edinburgh, 1972), p. 223.
9. B. L. Gledhill *et al.*, *J. Cell. Physiol.* **87**, 367 (1976).
10. M. A. Van Dilla *et al.*, *J. Histochem. Cytochem.* **25**, 763 (1977).
11. Available from Ortho Instruments, Westwood, Mass.
12. P. Dean, in *Flow Cytometry IV*, O. D. Laerum, T. Lindmo, E. Thorud, Eds. (Universitetsforlaget, Oslo, 1980), pp. 41–44.
13. D. Pinkel *et al.*, *J. Histochem. Cytochem.* **27**, 353 (1979). Under conditions where cell orientation works well, more than 90 percent of the sperm are properly oriented (*4*). The 0° detector alone is then adequate for accurate measurements.
14. Wild *M. oregoni* males were trapped for us by C. Rinaldo, Department of Zoology, Oregon State University. They were positively identified by their karyotypes, kindly done for us by S. Sherwood, and by the 9 percent split of the peaks in Fig. 2a. Other voles have much smaller DNA content differences between the sperm populations, as indicated by the karyotypes in T. C. Hsu and K. Benirschke, *An Atlas of Mammalian Chromosomes* (Springer-Verlag, New York, 1967–1977).
15. Work performed under the auspices of the U.S. Department of Energy by the Lawrence Livermore National Laboratory under contract number W-7405-ENG-48.

28 May 1982; revised 16 August 1982

Touching Textured Surfaces: Cells in Somatosensory Cortex Respond Both to Finger Movement and to Surface Features

Abstract. *Single neurons in Brodmann's areas 3b and 1 of the macaque postcentral gyrus discharge when the monkey rubs the contralateral finger pads across a textured surface. Both the finger movement and the spatial pattern of the surface determine this discharge in each cell. The spatial features of the surface are represented unambiguously only in the responses of populations of these neurons, and not in the responses of the constituent cells.*

The evolution in primates of the hand as a sensorimotor organ has doubtlessly contributed to the biological success of this order of mammals. One can trace through the prosimian and anthropoid primates an increasing capacity to manipulate, explore, and differentiate by touch objects and surfaces that are within reach (*1*). The unique tactile acuity of anthropoid primates, including man, depends in part on the high innervation density of the finger pads (*2*), but an important additional factor is the capacity to control and direct exploratory finger movements in resolving fine spatial features. Although one must normally rub the finger pads across a surface to identify it, the pattern of this exploratory movement may be varied greatly without impairing the tactile identification of the surface. From this it may be inferred that the neural representation of the spatial features of a surface at successive levels in the somatosensory pathways, although sustained by the movement of the finger pads across the surface, is largely independent of the actual pattern of finger movement.

We examined the tactile representation of simply patterned surfaces in Brodmann's areas 3b and 1 of the somatosensory cortex of the macaque. This region of cerebral cortex was chosen for analysis since its destruction, in both man and macaque, selectively impairs the subject's capacity to identify and differentiate textured surfaces with the contralateral fingers (*3*). Responses elicited in single cortical neurons when the monkey rubbed the finger pads to and fro across a ridged surface were recorded, and the effects of changing the spatial features of the surfaces touched and the pattern of finger movement used were studied systematically. The aim was to determine whether the spatial features of the surface were represented in these neural responses. A previous study (*4*) showed that the representation of these same spatial features in the monkey's digital nerve occurs only in the discharge of the population of mechanoreceptive fibers engaged by the patterned surface. Individual fibers in this population never specify the dimensions of the surface, since their responses depend not only on these dimensions but also on the pattern of movement of the skin relative to the surface. We found that this is also true for neurons in corti-

0036-8075/82/1126-0906$01.00/0

cal areas 3b and 1: the responses of the individual cortical neurons differed substantially from those of digital nerve fibers, but the stimulus factors determining their responses were similar. As in the digital nerve, within cortical areas 3b and 1 the independent representation of the spatial features of the surface explored with the fingers must occur in the response of the population of neurons.

Two male macaques (*Macaca nemestrina*) were trained to rub the finger pads of the hand across a particular surface and to use, upon request, both a particular sinusoidal pattern of finger movement and a particular contact force. This was achieved by training the monkeys to manually track a target displayed on an oscilloscope screen in front of them (Fig. 1). The monkeys accurately tracked sinusoidally moving targets with frequencies in the range 0.2 to 1.2 Hz, as shown in the middle column of Fig. 1 and in Fig. 2: the peak-to-peak amplitude of finger movement was 8 cm and the contact force was 30 to 80 g. The sinusoidal patterns of finger movement were chosen to match the finger movements that are often spontaneously selected by human subjects when differentiating textured surfaces (*5*).

The surfaces used were periodic gratings constructed by the photoetching of a rigid nylon base (*6*). Each surface was specified by its spatial period (3000, 1500, or 750 μm); the cycle profile was similar for all three surfaces (Fig. 1).

Responses of single neurons located in areas 3b and 1 of the postcentral gyrus were recorded daily over several weeks with platinum-iridium microelectrodes (*7*). In our sample 390 mechanoreceptive neurons had cutaneous receptive fields on the terminal phalanx of the second, third, or fourth digit. Of these, 76 were suitable for extended study; their receptive fields were located centrally on a terminal finger pad on skin with which the monkeys touched the grating. There were no systematic differences in the response characteristics of cells sampled in areas 3b and 1. More than 90 percent of the neurons receiving input from the finger pads had small, sharply bounded cutaneous receptive fields, 3 to 10 mm in diameter when plotted with a hog-hair brush. A few cells had larger cutaneous receptive fields extending over the glabrous and hairy skin of two phalanges. More than 80 percent of the neurons with small receptive fields were silent except when the skin in their receptive field was mechanically stimulated; nearly all of these cells adapted rapidly to steady indentation of the skin. The remaining neurons often had an ongoing discharge of 10 to 20 impulses per second and adapted slowly to sustained indentation of the skin.

All the neurons with receptive fields on the skin touching the gratings discharged when the monkeys rubbed the finger pads tangentially across this surface. The center column in Fig. 1 illustrates the discharge elicited in a cortical neuron in area 3b when the contralateral finger pads were rubbed to and fro across a grating: the cyclic movement was sinusoidal, with a fixed amplitude (8 cm, peak to peak) but changing frequency (0.3, 0.6, and 1.2 Hz). The cell's discharge was modulated in synchrony with the finger movement at each frequency. The cycle histogram in Fig. 1A illustrates this periodic discharge when the frequency of finger movement was 0.6 Hz: during each cycle the neuron was silent with the finger at rest, but discharged with movement of the finger in either direction. This pattern was observed in 13 of 76 neurons. The discharge in a more active neuron is shown in Fig. 1B. With a few neurons this discharge was significant only when finger movement was in one direction (Fig. 1C and Fig. 2D). The mechanism underlying this directional selectivity was probably peripheral: as the finger moved in one direction the receptive field zone was pressed firmly against the grating,

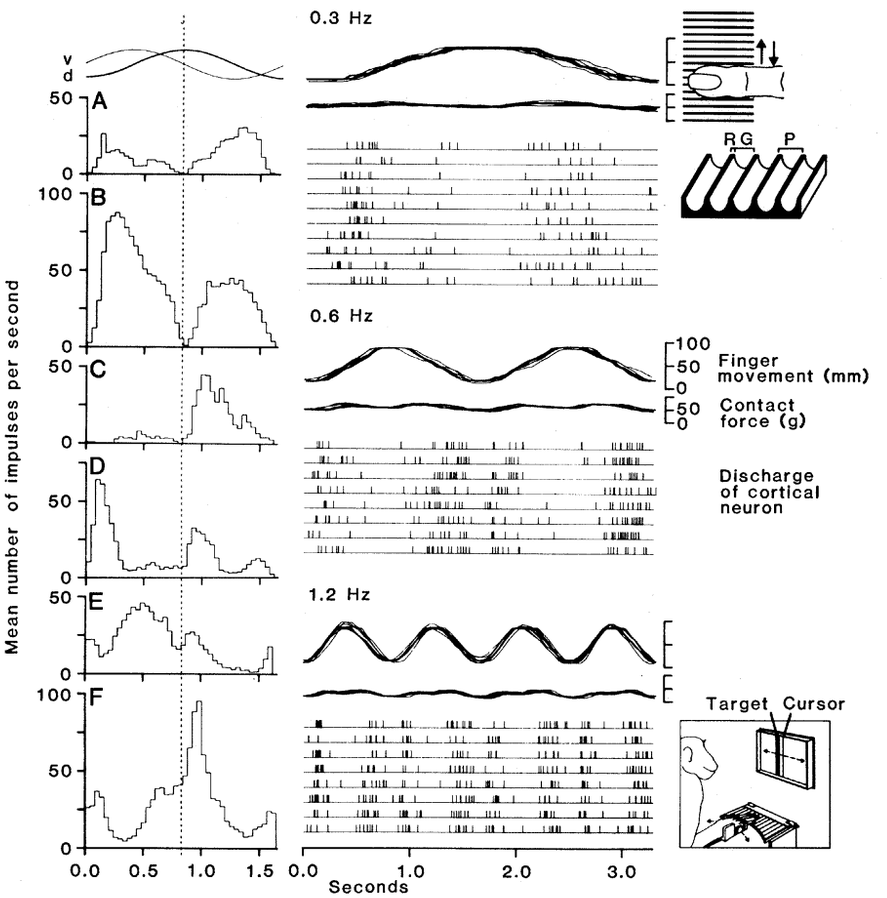

Fig. 1. Discharge patterns in cortical neurons in Brodmann's areas 3b and 1, elicited when a monkey rubbed the contralateral finger pads to and fro across a ridged surface (spatial period, 3000 μm; ridge : groove spatial ratio, 1:7). The macaque was trained to use, on request, a sinusoidal finger movement with a particular frequency and amplitude, and to maintain the contact force within a preset range (see cartoon at lower right). The monkey continuously superimposed the cursor line, which indicated the position of its fingers, on the moving target. The surface was a nylon grating (upper right). Column in center illustrates the discharge of a single neuron (diameter of receptive field, 5 mm) in area 3b, recorded while the monkey moved its third digit to and fro with frequencies of 0.3, 0.6, and 1.2 Hz and a fixed amplitude of 8 cm. In each block of data the upper traces indicate the position of the finger pad on the grating, the next sequence of traces indicates contact force, and the vertical bars indicate the occurrence of single action potentials recorded during these finger movements. The correlation between the finger movement and the cell's discharge is apparent. The cycle histogram in (A) is the averaged response of this neuron to 142 cycles of finger movement with a frequency of 0.6 Hz (bin width, 0.04 second). The remaining cycle histograms are the averaged responses (> 100 cycles) of other cortical neurons responding to the same sinusoidal finger movement. Each of these cells had a small receptive field on the distal pad of either the second or third digit. The cyclic change in finger position (*d*) and velocity (*v*) are plotted at top left. Dotted line indicates the midpoint of the cycle. Abbreviations: *P*, period; *G*, groove; and *R*, ridge.

whereas with movement in the reverse direction the same skin was lifted away from the surface.

Figure 1D illustrates the commonest pattern of discharge (41 of 76 cells) elicited in neurons of areas 3b and 1 by sinusoidal movement of a finger pad across a grating. Typically the cell discharged vigorously with the onset of finger movement, and often again when movement slowed. The asymmetry in the cyclic discharge shown in Fig. 1, D and E, was common. The peaks in this cyclic discharge occurred when acceleration or deceleration of the finger was near maximum.

In 9 of 76 cortical neurons examined systematically there was an ongoing discharge of 10 to 20 impulses per second. This discharge rate was modulated when the fingers were passed to and fro across the grating (Figs. 1F and 2C). The peak discharge now occurred close to the moment when the finger was at rest at the extremes of its movement. This response pattern suggested that moving the finger across the grating inhibited cell discharge, a view reinforced by the observation in five neurons that the mean impulse count during the period of cyclic movement was less while the pad was rubbed against the surface than when the skin was not stimulated. In addition, in two of these cells we identified distinctive excitatory and inhibitory regions in the receptive field. With most of the cortical neurons studied, the form of the modulated discharge measured by the cycle histogram (Fig. 2, A and B) did not change greatly with changes in the frequency of the finger movement.

We then measured the responses in cortical cells elicited by rubbing the fingers across gratings with different spatial periods (750, 1500, and 3000 μm). Frequencies of finger movement ranged from 0.3 to 1.2 Hz. Figure 2, A to D, illustrates the selective responsiveness of four of these neurons to gratings with periods of 3000 and 1500 μm. For most of the 29 cells studied the mean number of impulses per cycle was greater with the coarser grating (Fig. 2E). This increased response typically occurred during a limited segment of the cyclic response—for example, as the finger moved to the left (Fig. 2, A and B). In other neurons the increase in the response was general (Fig. 2C). We observed one neuron (Fig. 2D) that repeatedly responded vigorously to the 3000-μm grating but not to the finer grating with a spatial period of 1500 μm.

These experiments establish that when a monkey rubs its finger pads across a grating a population of previously silent neurons in contralateral cortical areas 3b and 1 discharge vigorously in synchrony with the finger movement. In addition, the responses of a significant proportion of these neurons change in an orderly way with changes in the spatial dimensions of the grating being explored. Since, however, the pattern of finger movement is incompletely represented in the cyclic discharge of any one cell, the spatial features of the grating are also incompletely specified by the responses of that cell. Populations of neurons responding to the grating contrast with their constituent cells in that both the finger movement and the spatial dimensions of the surface touched are specified with precision. How the different spatial

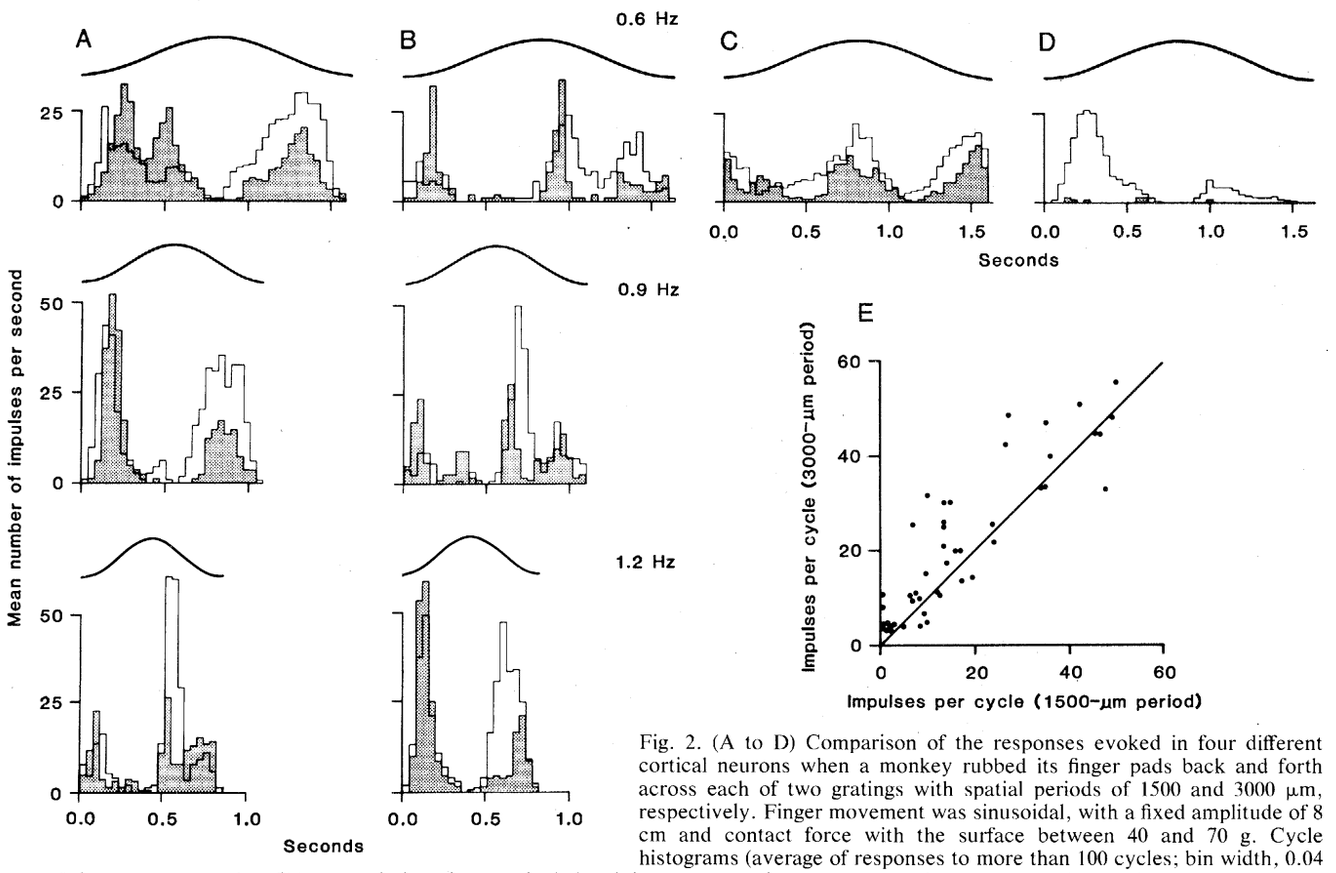

Fig. 2. (A to D) Comparison of the responses evoked in four different cortical neurons when a monkey rubbed its finger pads back and forth across each of two gratings with spatial periods of 1500 and 3000 μm, respectively. Finger movement was sinusoidal, with a fixed amplitude of 8 cm and contact force with the surface between 40 and 70 g. Cycle histograms (average of responses to more than 100 cycles; bin width, 0.04 second) for responses to the 1500-μm period grating are shaded and those representing responses to the 3000-μm period grating are unshaded. In (A) and (B) the responses elicited at different frequencies of finger movement (0.6, 0.9, and 1.2 Hz) are compared; in (C) and (D) the comparison is for finger movement with a frequency of 0.6 Hz. In all four neurons the average number of impulses elicited by a single cycle of finger movement was greater with the coarse grating. Commonly, this increase was within a specific segment of the cycle response (A and B), but the difference in the response to two gratings sometimes involved the entire cycle (C). (E) Mean cycle counts for 29 neurons responding to the two gratings (observations at two or three frequencies of finger movement for some cells). With each pair of responses the pattern of finger movement was similar. In most cases the cycle response was greater for the coarse grating than for the fine grating.

dimensions of a grating explored with the fingers are represented in the responses of cortical neurons remains to be determined.

Preliminary examination of neurons in area 2 (posterior to area 1) indicates that these cells differ substantially from those described above. Many area 2 cells had cutaneous receptive fields that responded to brushing of two or more adjacent finger pads but not of the intervening skin. A high proportion of these neurons responded vigorously to movement of the finger pads in one direction across a grating but not to movement in the reverse direction (*8*), and a further group of cells, although responding to repetitive, gentle brushing of the pads, did not respond when the pads were rubbed to and fro across the grating.

IAN DARIAN-SMITH
MICHIO SUGITANI
JOHN HEYWOOD
Sensory Processes Laboratory, Department of Physiology, University of Melbourne, Parkville, Victoria 3052, Australia
KEISHIRO KARITA
Department of Physiology, Tohoku University School of Dentistry, 4-1 Seiryo-machi, Sendai, Japan
ANTONY GOODWIN
Sensory Processes Laboratory

References and Notes

1. A. Bishop, in *Evolutionary and Genetic Biology of Primates*, J. Buettner-Janusch, Ed. (Academic Press, New York, 1964), pp. 133–225; J. R. Napier and P. H. Napier, *A Handbook of Living Primates* (Academic Press, London, 1967).
2. I. Darian-Smith and P. Kenins, *J. Physiol. (London)* **309**, 147 (1980); R. S. Johansson and A. B. Vallbo, *ibid.* **286**, 283 (1979).
3. E. Roland, *Arch. Neurol.* **33**, 543 (1976); J. Semmes, in *Handbook of Sensory Physiology*, vol. 2, *Somatosensory System*, A. Iggo, Ed. (Springer, New York, 1973), pp. 719–742; M. Randolph and J. Semmes, *Brain Res.* **70**, 55 (1974); J. Semmes, L. Porter, M. Randolph, *Cortex* **10**, 55 (1974).
4. I. Darian-Smith and L. E. Oke, *J. Physiol. (London)* **309**, 117 (1980); I. Darian-Smith, I. Davidson, K. O. Johnson, *ibid.*, p. 135.
5. J. W. Morley, A. W. Goodwin, I. Darian-Smith, *Exp. Brain Res.*, in press.
6. The subjective roughness of a periodic grating increases with its spatial period and the width of its grooves (Fig. 1) and decreases with increases in the width of its ridges [S. J. Lederman, *Percept. Psychophys.* **16**, 385 (1974); M. M. Taylor and S. J. Lederman, *ibid.* **17**, 23 (1975)].
7. The methods used for recording single neurons in the cerebral cortex of the alert macaque were similar to those used by several other laboratories [E. V. Evarts, *Methods Med. Res.* **11**, 241 (1966); V. B. Mountcastle, J. C. Lynch, A. Georgopoulos, H. Sakata, C. Acuna, *J. Neurophysiol.* **38**, 871 (1975)]. Recordings for the first few weeks were in the left hemisphere. After the transfer of learned movements to the left hand, recordings were continued in the right hemisphere.
8. Directionally selective neurons of this type have been observed in area 2 [J. Hyvarinen and A. Poranen, *J. Physiol. (London)* **283**, 523 (1978); Y. Iwamura and M. Tanaka, *Brain Res.* **150**, 662 (1978); E. P. Gardner and R. M. Costanzo, *J. Neurophysiol.* **43**, 420 (1980)].
9. Supported by grants from the University of Melbourne, the National Health & Medical Research Council of Australia, the Ian Potter Foundation, and the Van Cleef Foundation.

14 July 1982

Manipulation of Event-Related Potential Manifestations of Information Processing Stages

Abstract. *The timing of two event-related potential components was differentially affected by two experimental variables. The earlier component (N_A) was affected by degradation of the stimuli and the later component (N2) by the nature of a classification task. The results support the hypothesis that N_A and N2 reflect sequential stages of information processing, namely, pattern recognition and stimulus classification.*

The identification of brain activity associated with sequential stages of information processing has broad significance for cognitive science. An assumption underlying the concept of sequential stages of processing is that the time required for an earlier stage to extract the information necessary for the operations of a later stage should affect the timing of the later stage. Also, the duration of a later stage may vary with the task being performed even though the durations of earlier stages remain constant (*1*). We report here a pattern of results compatible with these assumptions concerning the timing of two event-related potential (ERP) components believed to be associated with two sequential stages of processing.

There is now substantial evidence that the N2 component reflects discrimination and classification of stimuli (*2*). The peak latency of N2 varies as a function of the difficulty of discrimination and precedes and correlates with the timing of discriminative behavioral responses (*3*). In a recent study (*4*), we identified an earlier negative component (designated N_A) which seems to be associated with pattern recognition processes. On the basis of changes in the relative timing of these two components across experimental conditions, we inferred that the discrimination and classification processes associated with N2 depended on the prior stimulus identification processes associated with N_A.

We have now tested the hypotheses about the stages of information processing associated with N_A and N2 by differentially manipulating their timing. We predicted that degrading the stimuli would increase the peak (but not the onset) latency of N_A. Since we hypothesized that the processing associated with N2 depends on the processing associated with N_A, changes in the peak latency of N_A should affect the timing of N2. On the other hand, varying the time required to perform a classification task was expected to affect only the peak latency of N2, producing an increase in the interval between the peaks of N_A and N2.

Eleven adult subjects were given two

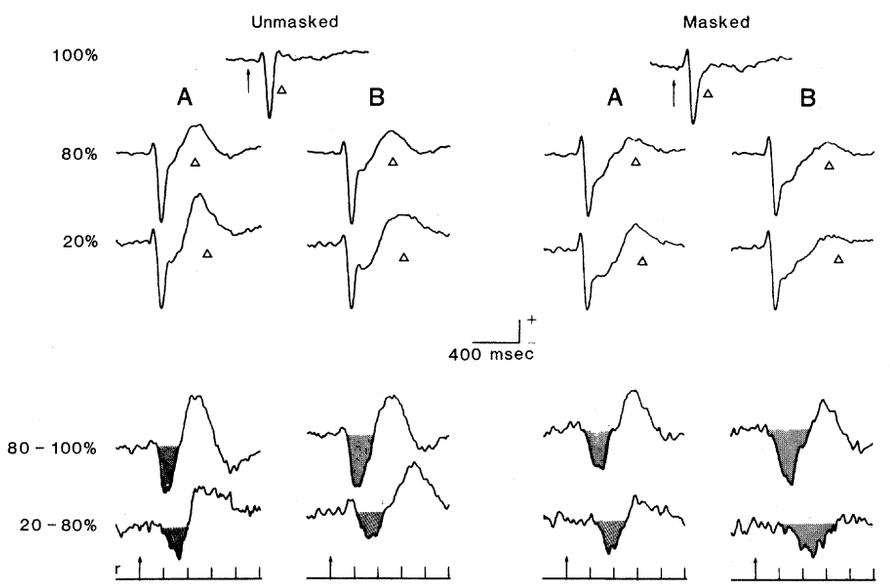

Fig. 1. Grand mean waveforms (11 subjects) at T5 to the unmasked and masked stimuli in tasks A and B during simple RT (100 percent) and choice RT (80 and 20 percent). Dark areas in difference waveforms below indicate N_A (80 − 100 percent) and N2 (20 − 80 percent). The bottom right waveform is from seven subjects for whom N2 could be measured in that condition. Arrows indicate stimulus onset and open triangles indicate mean RT. Voltage calibration is 5 μV for the upper three rows and 2.5 μV for the difference waveforms.

0036-8075/82/1126-0909$01.00/0